Chemical and Process Engineering: New Frontiers, 2023, 44(4), e44
DOI: 10.24425/cpe.2023.147403

High-temperature and mechanochemical synthesis of Sm_5VO_{10} and its unknown properties

Kamil Kwiatkowski*, Mateusz Piz, Elżbieta Filipek

West Pomeranian University of Technology in Szczecin, Faculty of Chemical Technology and Engineering, Piastów 42, 71-065 Szczecin, Poland

*** Corresponding author:**
e-mail:
kamil.kwiatkowski@zut.edu.pl

Article info:
Received: 12 May 2023
Revised: 02 August 2023
Accepted: 04 September 2023

Abstract
In the presented work, the conditions of the high-temperature and mechanochemical method for the synthesis of compound Sm_5VO_{10} and their influence on its physicochemical properties were studied. The following methods were used for the study: X-ray powder diffraction (XRD), differential thermal analysis (DTA), infrared spectroscopy (FTIR), ultraviolet and visible light spectroscopy (UV–VIS–DRS), scanning electron microscopy (SEM-EDX), and laser beam diffraction spectrometry (LDS). Based on the results, it was determined that the compound Sm_5VO_{10} is thermally stable in air atmospheres up to 1475 °C, crystallises in a monoclinic system, and its structure is made up of oxygen VO_4 and SmO_8 polyhedra. The estimated energy gap value for nanometric, mechanochemically obtained Sm_5VO_{10} was about 3.20 eV, and for the microcrystalline, obtained with the high-temperature method, was about 2.75 eV. The established physicochemical characterisation of Sm_5VO_{10} initially showed that the compound could find potential applications, e.g. as a photocatalyst for water purification or as a component of new optoelectronic materials.

Keywords
high temperature and mechanochemical synthesis, Sm_5VO_{10} compound, thermal stability, XRD, semiconductor

1. INTRODUCTION

For several decades, intensive, interdisciplinary research has been focused on the search for new advanced, functional materials that are and will always be essential for human progress. Such materials, combined with the technologies developed to produce them, provide efficient and sustainable solutions to meet future societal challenges. Among the new materials being explored, those whose components contain compounds and/or solid solutions of rare earth elements (REEs) occupy an important place. It is well known (Balaram, 2019) that these elements give materials unique optical, electronic and magnetic properties, making them valuable for many modern applications. Among the various compounds, metal vanadates(V) in particular – and REEs in particular – represent an interesting class of compounds due to their wide range of possible applications, from catalysis, electronics and optoelectronics to painting. For example, bismuth(V) orthovanadate(III) is commercially available as a yellow pigment (Dunkle et al., 2009), and yttrium orthovanadate(V) doped with neodymium ions has found applications as a crystal laser used for optical imaging in medical diagnostics (Gao and Wong, 2014). Moreover, recently holmium, yttrium and dysprosium orthovanadates(V) have found use as components of electrodes for quantification of pharmaceuticals (Sriram et al., 2023).

Despite the considerable progress of research focused on the methods of synthesis and properties of REE vanadates(V), there is still a lot of information that needs to be verified or even supplemented. In particular, data is missing about the crystal structure or thermal stability of still little understood representatives of this group of compounds.

Unlike the orthovanadates(V) of the rare earth elements ($REVO_4$), which are well described in the literature, by far the least described family of vanadates(V) are the compounds with general formulae $RE_8V_2O_{17}$ and $RE_{10}V_2O_{20}$ (RE_5VO_{10}) (Brusset et al., 1971; Kitayama and Katsura, 1977; Yamaguchi et al., 1989). Thus, among the compounds formed in the V_2O_5–Sm_2O_3 binary system, samarium(III) orthovanadate(V)–$SmVO_4$ is extensively characterized (Denisova et al., 2015; Ge et al., 2018; Li et al., 2013), while the existence of the compounds $Sm_8V_2O_{17}$ and Sm_5VO_{10} has only been hinted at.

Due to only residual or even missing information on alternative methods of synthesis and physicochemical properties of such vanadates(V) of various rare earth elements, it is necessary to expand the state of knowledge about these families of compounds. Learning about the properties of such compounds, as well as the solid solutions of which they are matrixes, is essential for developing new materials with desirable and designable properties.

This paper presents the results of research into synthesis methods, the crystal structure and unknown physicochemical properties, including potential areas of application for the only signalled in the bibliography samarium(III) vanadate(V) with the formula Sm_5VO_{10} (Brusset et al., 1971; Kitayama and

Katsura, 1977). From the literature data on this compound, it is only known to form in a reaction between vanadium(V) oxide and samarium(III) oxide.

2. EXPERIMENTAL

2.1. Materials and synthesis

In order to obtain the compound Sm_5VO_{10} with high-temperature solid state reactions in an air atmosphere, a mixture was prepared from the oxides, i.e. vanadium(V) oxide and samarium(III) oxide, with a molar ratio of V_2O_5 : Sm_2O_3 equal to 1:5. A mixture of Sm_2O_3 with separately obtained $SmVO_4$ was also prepared (Denisova et al, 2015), with a molar ratio of 2:1. A mixture of oxides with a molar ratio of V_2O_5 : Sm_2O_3 of 1:5 was prepared for synthesis by milling (mechanochemical).

Vanadium pentoxide and samarium sequioxide (both analytical pure, Alfa Aesar, Germany) were used for the syntheses. XRD analysis of the substrates revealed the presence of rhombohedral V_2O_5 (PDF card number 04-008-7123) and Sm_2O_3, which is a mixture of regular (PDF card number 04-002-5117) and monoclinic Sm_2O_3 (PDF card number 04-004-2795). In order to remove samarium(III) hydroxide present in small amounts in commercial samarium(III) oxide, this substrate was annealed for 3 hours at 600 °C. Below this temperature, $Sm(OH)_3$ decomposes to Sm_2O_3, as reported in the literature (Rahimi-Nasrabadi et al., 2017).

2.2. Sample preparation

The compound Sm_5VO_{10} was synthesised using a high-temperature method by heating a mixture of oxides (Sm_2O_3 and V_2O_5) in six 12-hour steps:

$$\mathrm{I}: 600\,^{\circ}\mathrm{C} \rightarrow \mathrm{II}: 620\,^{\circ}\mathrm{C} \rightarrow \mathrm{III}: 630\,^{\circ}\mathrm{C} \rightarrow \mathrm{IV}: 800\,^{\circ}\mathrm{C} \rightarrow \mathrm{V}: 1250\,^{\circ}\mathrm{C} \rightarrow \mathrm{VI}: 1350\,^{\circ}\mathrm{C}.$$

In contrast, this compound from a mixture of samarium(III) oxide and $SmVO_4$ was obtained only in three 12-hour steps at temperatures of: 1000 °C (2×) and 1350 °C. The synthesis with the mechanochemical method was carried out in three steps: 2 × 550 RPM (3 h), 1 × 600 RPM (1 h), in a reactor (PULVERISITTE 6, Fritsch) made of zirconium oxide ZrO_2 of 250 cm^3 volume and maintaining a BPR (ball to powder ratio) equal to 20:1. 46 balls 20 mm in diameter were used.

2.3. Characterization of the samples

Table 1 gives the instrumental methods and measurement conditions. X-ray diffraction (XRD) was used to observe changes in the phase composition of the samples, after different stages of heating or milling. To study selected physicochemical properties of the resulting product, the following methods were used: gas ultrapycnometry, differential thermal analysis combined with thermogravimetry (DTA-TG), ultraviolet and visible light diffuse reflectance spectroscopy (UV–VIS–DRS), Fourier-transform infrared spectroscopy (FTIR), laser diffraction spectrometry (LDS) and scanning electron microscopy with energy-dispersive X-ray spectroscopy (SEM-EDX).

Table 1. Instrumental methods and conditions of measurements.

Method	Apparatus	Measurement conditions
XRD	Empyrean II (PANalytical, Netherlands)	CuK_α ($\lambda = 1.5418$ nm) Graphite monochromator 2θ range 7–45 ° time of counting 150.45 s
Gas ultrapycnometry	Ultrapyc 1200e (Quantachrome Instruments, USA)	Argon, 99.999% (5N)
DTA–TG	Discovery SDT 650 (TA Instruments Co., USA)	Heating rate 10 deg/min Range 20–1300 °C Air atmosphere Sample mass about 30 mg
UV–VIS–DRS	V-670 (JASCO, Japan)	Range 200–800 nm Integrating sphere PIV-756/PIN-757 Calibrated on $BaSO_4$
FTIR	Nicolet iS5 (ThermoFisher, USA)	Range 400–4000 cm^{-1} Dilution 1:300 in KBr
LDS	Mastersizer 3000 (Malvern Panalytical, UK)	He–Ne laser (λ =632.8 nm) LED ($\lambda = 470.0$ nm)
SEM–EDX	SU-70 (Hitachi, Japan)	Accelerating voltage 5–15 kV Spectrometer EDX NORAN™ System 7 (Thermo Fisher Scientific)

Identification of the phases present in the samples after successive synthesis steps was based on the data contained in PDF cards from the ICDD PDF4+ database and literature data (Brusset et al., 1971; Kitayama and Katsura, 1977).

3. RESULTS AND DISCUSSION

The study started with the synthesis of Sm_5VO_{10} from oxides by annealing a mixture of Sm_2O_3 and V_2O_5 (5:1) at 600 °C for 12 h. The temperature of the first heating step was determined from the result of DTA-TG analysis of a mixture with a composition of 16.67% mol of V_2O_5 and 83.33% mol of samarium(III) oxide (Fig. 1).

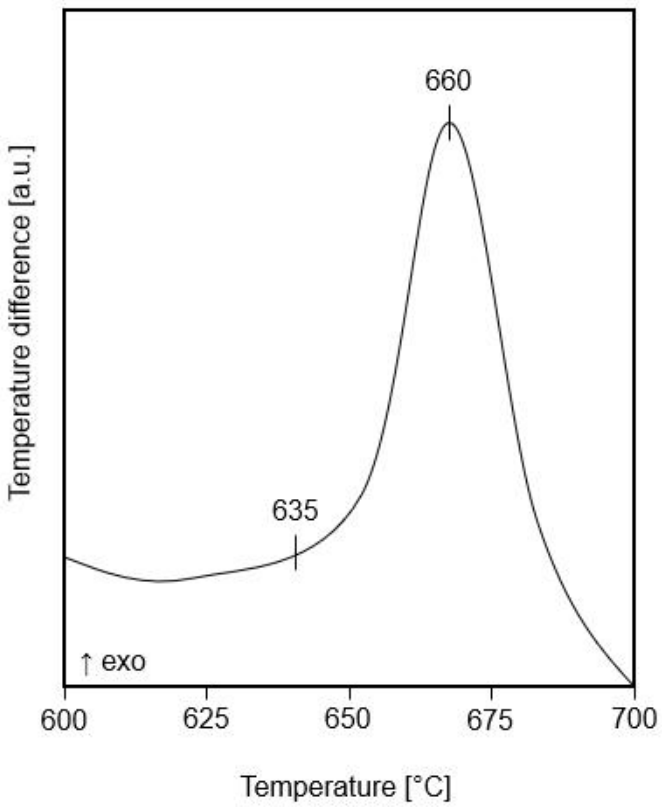

Figure 1. Part of a DTA curve of an oxide mixture containing 16.67% mol of V_2O_5 and 83.33% mol of samarium(III) oxide.

In the DTA curve (Fig. 1) in the temperature range 20–1000 °C, only one well-developed exothermic effect was recorded, with an onset temperature of about 635 °C and a maximum at about 660 °C. This effect is related to the reaction occurring between the oxides, resulting in the formation of samarium(III) orthovanadate(V), which was confirmed by examining the phase composition (XRD) of the analysed mixture after its DTA measurement up to 1000 °C. Furthermore, the temperature of the first heating stages of the sample (I–III) was chosen so that the vanadium(V) oxide or the eutectic mixture formed with it did not melt, i.e. below 675 °C (Remizov et al., 1976).

After the first heating step (600 °C) of the oxide mixture, the diffractogram of the sample showed reflections next to the diffraction lines belonging to the substrate set, which were assigned to $SmVO_4$ based on PDF4+ database (PDF card no. 04-012-7513). The further two stages of sample roasting, i.e. at 620 °C (12 h) and 630 °C (12 h), resulted in a biphasic sample containing only $SmVO_4$ and Sm_2O_3 (Fig. 2). Due to the high melting points of the phases present in the sample, ($T_{Sm2O3} = 2335$ °C, $T_{SmVO4} \geq 1440$ °C), the sample was heated at higher temperatures, i.e. 800 (12 h), 1250 (12 h) and 1350 °C (12 h). Fig. 2 shows sections of diffractograms of the synthesised sample, before and after selected heating steps, i.e. after which its phase composition changed significantly.

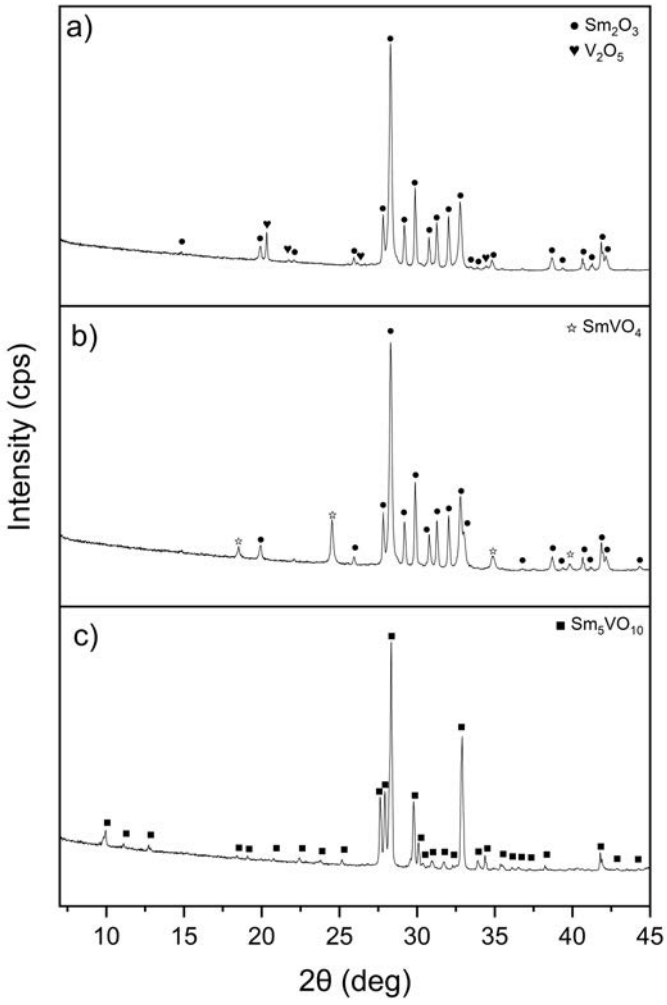

Figure 2. Fragments of sample diffractograms, before and after selected stages of its heating: a) substrate mixture; b) after the 3rd stage 630 °C (12 h); c) after the last stage 1350 °C (12 h).

Heating the sample at 800 °C (12 h) did not result in significant changes in its phase composition and, therefore, in the next stage of its heating, the temperature was increased to 1250 °C. Heating the sample at this temperature for 12 h resulted in the observation in its diffractogram, besides XRD lines belonging to the $SmVO_4$ and Sm_2O_3 sets, those which, according to the literature (Brusset et al., 1971; Kitayama and Katsura, 1977), were attributed to the compound Sm_5VO_{10} (PDF card no. 00-031-1219), as well as additional ones that were not included in this card. These additional XRD reflections did not belong to any of the phases that can form in the V_2O_5–Sm_2O_3 system. Further heating of the sample at the same temperature over 12 h resulted in a decrease in the intensity of the diffraction lines originating from $SmVO_4$ and Sm_2O_3. At the same time, an increase in the intensity of lines from Sm_5VO_{10} was observed in the diffractograms, including additional lines. Heating the sample at 1350 °C (12 h) resulted in a sample that was monophasic and contained only the compound Sm_5VO_{10} (Figure 2).

Analysis of the phase composition of the test sample after successive heating steps clearly showed that the synthesis of the compound Sm_5VO_{10} occurs via an intermediate step, in which samarium(III) orthovanadate(V) is formed according to Reaction (1).

$$Sm_2O_{3(s)} + V_2O_{5(s)} = 2SmVO_{4(s)} \quad (1)$$

Subsequently, formed $SmVO_4$ reacts with the Sm_2O_3 contained in the reaction mixture in excess of orthovanadate's stoichiometry, to form the compound Sm_5VO_{10} (Reaction 2).

$$SmVO_{4(s)} + 2Sm_2O_{3(s)} = Sm_5VO_{10(s)} \quad (2)$$

The set of diffraction lines collected after the last heating step of the samples differed significantly from that known from the literature (Brusset et al., 1971; Kitayama and Katsura, 1977), i.e. it was richer by many lines, and the mutual relations of their intensities were also different.

To confirm the formation of Sm_5VO_{10} following the reaction between samarium(III) orthovanadate(V) and Sm_2O_3, a sample containing 33.33% mol of $SmVO_4$ in a mixture with samarium(III) oxide was prepared. Due to the high thermal stability of both substrates, heating of the sample started at 1000 °C. As in the sample prepared from the oxides, a decrease in the intensity of the diffraction lines from the substrates and a simultaneous increase in the intensity of the lines from Sm_5VO_{10} were observed in its diffractogram after this heating step (Fig. 3). Fig. 3 shows a summary of the diffractogram fragments before, after the first and last heating step of the sample.

The diffractogram of this sample after the last synthesis stage, that is 1350 °C (6 h) (Fig. 3) was similar to the spectra of Sm_5VO_{10} obtained from the oxides mixture (Fig. 2), which additionally confirmed the forming of samarium(III) vanadate(V).

Due to the significant differences between the test results obtained and the data available in the literature (Brusset et al., 1971; Kitayama and Katsura, 1977), as well as the lack of information on the structure of Sm_5VO_{10}, the next stage of the study was to establish its basic crystallographic data. For this purpose, the diffractogram of a single-phase sample containing Sm_5VO_{10} was indexed with the experimentally determined density of Sm_5VO_{10}. The samarium(III) vanadate(V) density value was determined using the gas ultrapicnometry method. The determined value of the density of Sm_5VO_{10} was 6.46 ± 0.05 g/cm^3. The 15 most intense XRD lines from the 2θ range from 4 to 90° were selected for indexing using POWDER program. A range of solutions was obtained, of which the best agreement with the experimental data was shown by the primitive monoclinic unit cell model. The best results obtained from Sm_5VO_{10} indexing are shown in Table 2.

According to the indexing results it was calculated that:

- Unit cell parameters are as follows: $a = 0.9041$ nm, $b = 0.8022$ nm, $c = 1.3239$ nm, $\alpha = \gamma = 90.0000°$, $\beta = 90.7148°$;
- Volume of the unit cell $V = 0.9601$ nm^3;
- Number of molecules in the unit cell $Z = 4$;
- Theoretical density $d = 6.66$ g/cm^3.

The high values of quality coefficients for each XRD line of the chosen solution and the good agreement of the X-ray density with the experimentally determined one indicate a high probability of the correctness of the chosen solution.

The next stage of the research was an attempt at the synthesis of Sm_5VO_{10} with the mechanochemical method. For this purpose, a sample containing 16.67% mol of V_2O_5 mixed with samarium(III) oxide was prepared and subjected to a three-stage grinding in a high-energy planetary ball mill. The conditions for the synthesis carried out with the method are given in the experimental part. They were established after analysis of data given in the literature (Filipek and Wieczorek-Ciurowa, 2009; Malicka et al., 2020; Piz et al., 2018; Tojo et al., 2007; Zhang and Saito, 2000; Zhang and Saito, 2012) about mechanochemical synthesis of various phases formed in binary systems. Moreover, the mechanisms of the process (not analyzed in this paper) are well described, for example in the paper (Baláž et al., 2013).

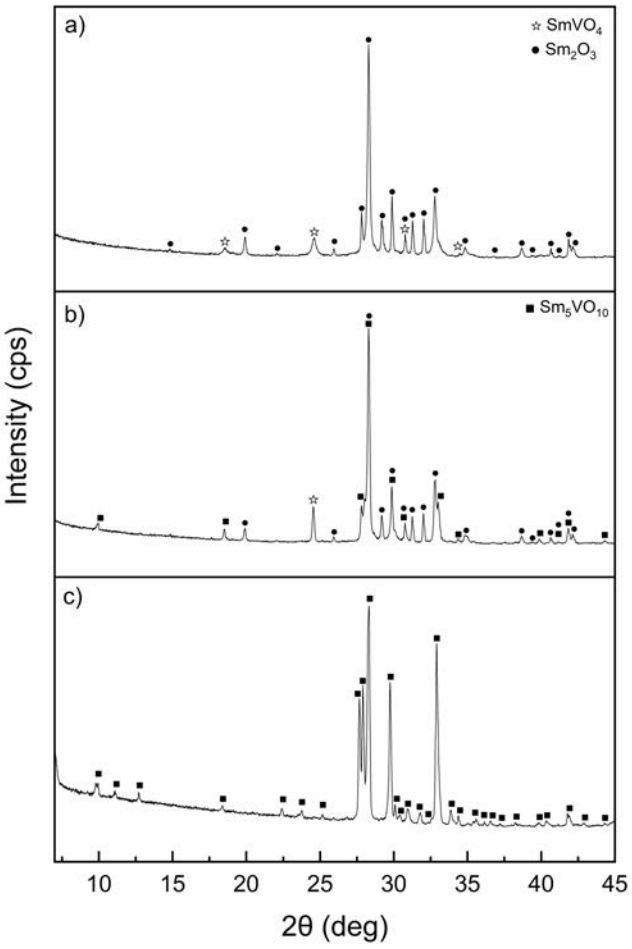

Figure 3. Fragments of sample diffractograms: a) substrate mixture ; b) after the 1st stage 1000 °C (12 h) ; c) after the last stage 1350 °C (6 h).

Table 2. Results of indexing powder Sm_5VO_{10} diffractogram.

No.	*hkl*	d_{obs} [nm]	d_{cal} [nm]	I/I_0 [%]
1	1 0 0	0.9044	0.9041	20
2	0 1 0	0.7978	0.8022	13
3	0 1 –1	0.6965	0.6899	12
4	1 0 3	0.3965	0.3965	7
5	1 2 –2	0.3228	0.3223	87
6	1 2 2	0.3196	0.3192	95
7	2 0 2	0.3161	0.3158	100
8	2 2 0	0.3000	0.3000	78
9	2 2 –1	0.2940	0.2932	6
10	1 1 4	0.2890	0.2887	9
11	3 1 0	0.2817	0.2821	9
12	2 2 2	0.2722	0.2723	98
13	0 0 5	0.2644	0.2648	7
14	0 3 –1	0.2625	0.2627	2
15	4 1 –1	0.2152	0.2148	4

Phase analysis (XRD) after the first grinding step (550 RPM, 3 h) of the mixture of V_2O_5 with Sm_2O_3 showed that in addition to Sm_2O_3 oxide, the compound $Sm_8V_2O_{17}$ was probably present in the sample. This means that V_2O_5 contained in the reaction mixture reacted completely with Sm_2O_3 in accordance with Reaction (3) to form $Sm_8V_2O_{17}$, i.e. a compound whose existence was so far signalized only in a few papers (Brusset et al., 1971; Kitayama and Katsura, 1977).

$$4Sm_2O_{3(s)} + V_2O_{5(s)} = Sm_8V_2O_{17(s)} \quad (3)$$

However, at this stage of research, it cannot be ruled out that $SmVO_4$ is formed in situ in the reaction mixture, which reacts with Sm_2O_3 to $Sm_8V_2O_{17}$.

$$2SmVO_{4(s)} + 3Sm_2O_{3(s)} = Sm_8V_2O_{17(s)} \quad (4)$$

The second stage of milling, under the same conditions, did not significantly change the phase composition of the sample, and therefore in the third stage of the mechanochemical synthesis, the RPM was increased to 600 and the time of synthesis of the title phase was reduced to 1 hour.

A diffractogram of the sample after the third milling step registered few intense lines, which could not be attributed to the substrates, i.e. V_2O_5 and Sm_2O_3 as well as to $Sm_8V_2O_{17}$ and $SmVO_4$, but only to samarium(III) vanadate(V)–Sm_5VO_{10}. It can therefore be concluded that in this milling step a reaction took place according to Equation (5).

$$Sm_8V_2O_{17(s)} + Sm_2O_{3(s)} = 2Sm_5VO_{10(s)} \quad (5)$$

The phase composition of this sample did not change after extending the time of its grinding under these conditions up to 10 h.

Figure 4 shows a summary of diffractograms of the sample, before milling and after the final synthesis step.

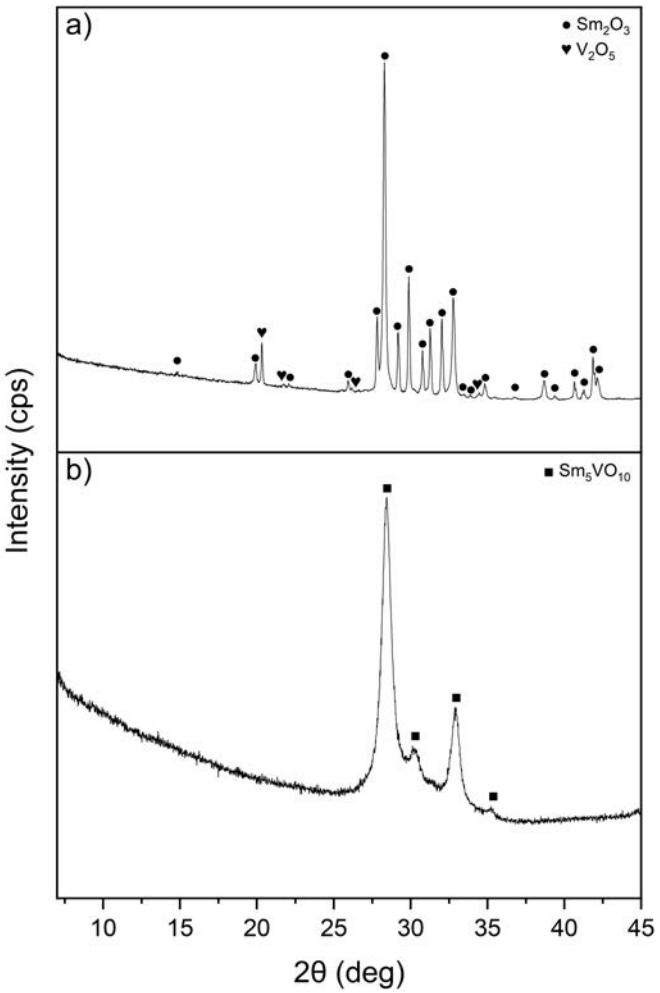

Figure 4. Fragments of diffractograms of the sample a) before synthesis; b) after the 3rd grinding (600 RPM 1 h).

The broadened diffraction lines in the diffractogram of the Sm_5VO_{10} obtained with the mechanochemical method indicate that the obtained crystallites of the compound are nanometric in size. Absence of some XRD lines, according to the diffraction spectra obtained with the high temperature method, as well as high background indicate, that the amorphous phase is present in the product.

At this stage of research, it cannot be excluded that the amorphous phase is the compound Sm_5VO_{10}. This assumption is supported by the research results presented in the further part of this paper.

The sizes of the crystallites of the synthesised Sm_5VO_{10}, were determined with the Scherrer method (Patterson, 1939). Their average size was calculated to be approximately 7.5 nm and did not significantly change after 10 h of milling. However, the unit cell parameters of the compound obtained mechanochemically were not calculated due to the insufficient number of XRD lines for the monoclinic crystallographic system.

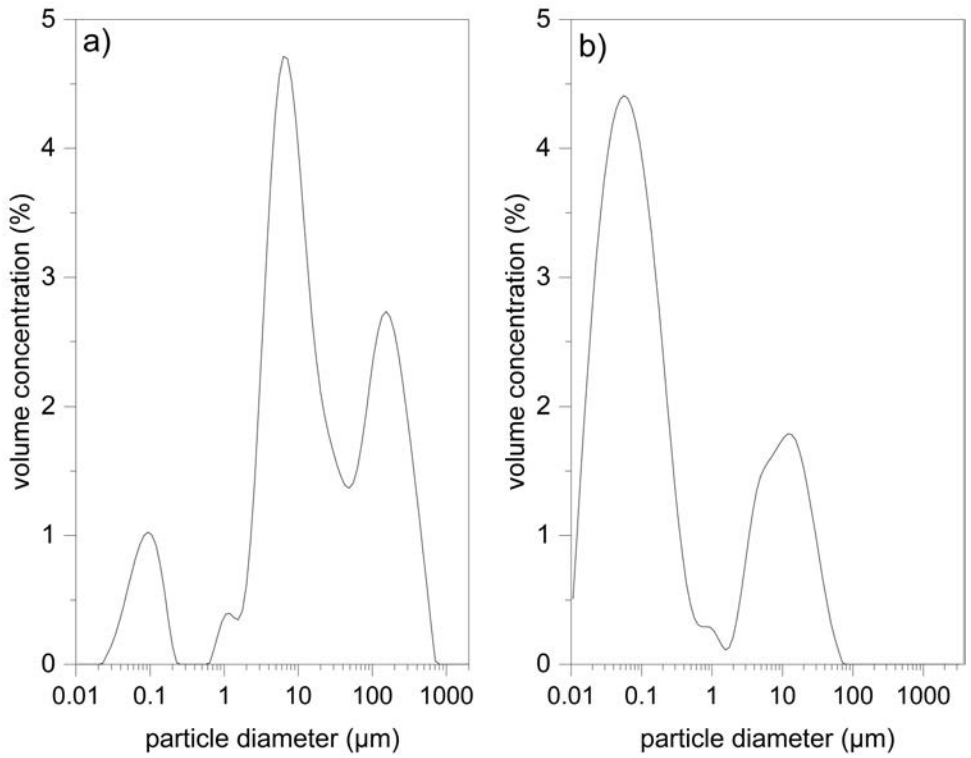

Figure 5. Average particle size distribution curve of obtained Sm_5VO_{10} with the methods a) high temperature; b) mechanochemical.

In the next stage of the study, the average particle size distribution of the compound Sm_5VO_{10} obtained with both high-temperature and mechanochemical methods was determined using LDS method (Fig. 5).

Based on LDS analysis of Sm_5VO_{10} obtained with the high-temperature method, the sizes of the crystallites were micrometre-sized and mostly ranged from 7 to 153 μm. In contrast, most crystallites of the product obtained with high-energy ball milling have sizes below 60 nm, including ∼ 10% below 23 nm. At this stage of research, it is not possible to explain why the micrometric fraction is present in this sample. It cannot be excluded that this is due to the agglomeration of particles.

For the crystallites of the compound that were synthesised with both methods, their sizes were estimated from SEM-EDX studies (Fig. 6).

The crystallites of pentasamarium decaoxovanadate (Sm_5VO_{10}) have the shape of irregular polyhedrons and, depending on the synthesis method, their sizes range from 0.5 to ∼ 3 μm in the case of high-temperature synthesis (Fig. 6a) and from ∼ 50 nm to 200 nm – in the case of mechanochemical synthesis (Fig. 6b). The differences in the determined crystallite size values are due to measurement errors of the used test methods. This does not change the overall conclusion that the product obtained mechanochemically is nanometric, and it is micrometric using the high-temperature method.

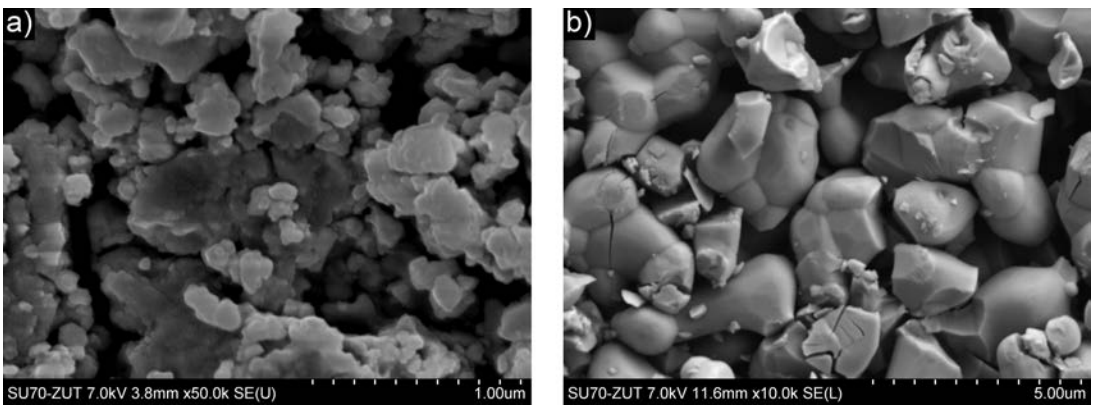

Figure 6. SEM images of Sm_5VO_{10} compound obtained with the methods: a) high-temperature, b) mechanochemical.

During SEM studies, EDX analysis was also carried out on the metallic elemental content of the Sm_5VO_{10} compound obtained in the air atmosphere with both methods. The results of the analysis are shown in Table 3.

The results of the analysis revealed that the atomic concentrations of vanadium and samarium are only slightly different from the theoretical values calculated for the percentage of individual metal atoms in Sm_5VO_{10} and are within the measurement error of $\sim$ 1% at. The results obtained confirm the validity of the assumed sum formula of the synthesized compound.

In order to initially determine from which oxygen polyhedra of vanadium and samarium the structure of the obtained compound Sm_5VO_{10} is composed, infrared spectroscopy studies were carried out. A comparative analysis of the IR spectrum of the mixture of V_2O_5 and Sm_2O_3 oxides with the IR spectra of the products obtained with the two methods from such a mixture allowed to conclude that these spectra differ significantly both in the position of the absorption bands and in their intensities. A comparison of the fragments of these IR spectra in the 400–1200 cm^{-1} range is shown in Figure 7.

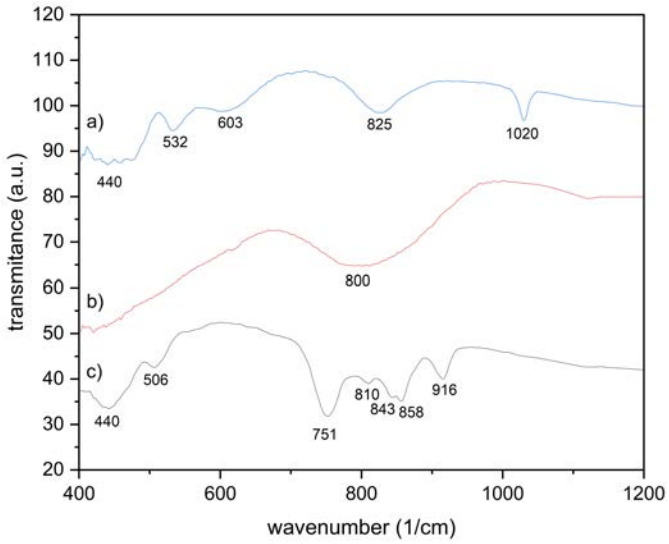

Figure 7. Fragments of the IR spectra of the: a) mixture of substrates; compound Sm_5VO_{10} obtained with the methods: b) mechanochemical, c) high-temperature.

The IR spectrum of the substrate mixture (Figure 7a) consists of absorption bands that, according to the literature data (Frederickson and Hausen, 1963; Gao et al., 2003) correspond to the stretching vibrations of the V–O and Sm–O bonds in the polyhedra of these metals. Thus, the absorption bands with maxima recorded at 825 and 1020 cm^{-1} are related to the vibrations of the V–O bonds, and from the Sm–O bonds come the bands at 603, 532 and 440 cm^{-1}. The spectrum of the compound Sm_5VO_{10} obtained with the mechanochemical method (Fig. 7b), consists of only one broad band with a maximum at 800 cm^{-1}. Due to the proportion of the amorphous phase in the sample obtained after mechanochemical synthesis, its IR spectrum (Fig. 7b) differs significantly from that of Sm_5VO_{10} obtained with the high-temperature method (Fig. 7c), mainly due to the lack of a fully formed crystal structure, i.e. only partial long-range ordering.

The IR spectrum of samarium(III) vanadate(V) obtained with the high-temperature method consists of seven absorption bands, with maxima indicating the presence of both VO_4 polyhedra (1000–700 cm^{-1}) and SmO_8 polyhedra (500–400 cm^{-1}) in the structure of this compound. By analogy with compounds formed in other systems, e.g. in V_2O_5–Y_2O_3 (Yamaguchi et al., 1989) or in V_2O_5–Yb_2O_3 (Piz and Filipek, 2017), it was found that Sm_5VO_{10} is built from VO_4 tetrahedra (Au et al., 1996) and SmO_8 dodecahedra (Chakoumakos et al., 1994; Huang et al., 2020). Due to the unknown full crystal structure of the studied compound and due to the fact that only qualitative evaluation of IR spectra was possible, it cannot be excluded that SmO_6 octahedra are also present in the structure of this compound.

Due to the lack of literature reports on the thermal stability of Sm_5VO_{10}, the next step of the study was to determine the temperature and way of melting of samarium(III) vanadate(V). Both the temperature and mode of melting were determined with XRD analysis conducted after successive 6-hour heating steps of a single-phase sample containing Sm_5VO_{10} in the temperature range from 1375 to 1475 °C. The temperature of successive heating stages of this sample was raised by 25 °C. A change in its phase composition was found only after heating it at 1475 °C. XRD analysis showed that the sample was three-phase and contained not only Sm_5VO_{10}, but also Sm_2O_3 and the compound $Sm_8V_2O_{17}$. The presence of the latter compound was found on the basis of its XRD characterization

Table 3. Results of the EDX analysis.

Element	Atomic concentration of elements in Sm_5VO_{10} obtained with high-temperature method [% at]	Atomic concentration of elements in Sm_5VO_{10} obtained with mechanochemical method [% at]	Calculated value from the formula Sm_5VO_{10} [% at]
V	16.20	17.37	16.67
Sm	83.80	82.45	83.33

provided only in the paper (Brusset et al., 1971). The sample did not melt after heating at this temperature, which made it possible to conclude that the tested compound Sm_5VO_{10} does not melt but decomposes into a solid state in an air atmosphere according to Equation (6).

$$2Sm_5VO_{10(s)} = Sm_8V_2O_{17(s)} + Sm_2O_{3(s)} \quad (6)$$

Moreover, the decomposition reaction was found to start at 1475 °C and occur at a low rate. An analogous decomposition reaction was described in the literature (Yamaguchi et al., 1989) for the compound Y_5VO_{10} formed in the binary V_2O_5–Y_2O_3 oxide system.

In the final step of the study, the energy gap value was estimated for the compound Sm_5VO_{10} synthesised with both methods, using the Kubelka–Munk transformation of the reflection spectrum obtained with the UV–VIS–DRS method (Kubelka and Munk, 1931). The transformed spectra are shown in Figure 8.

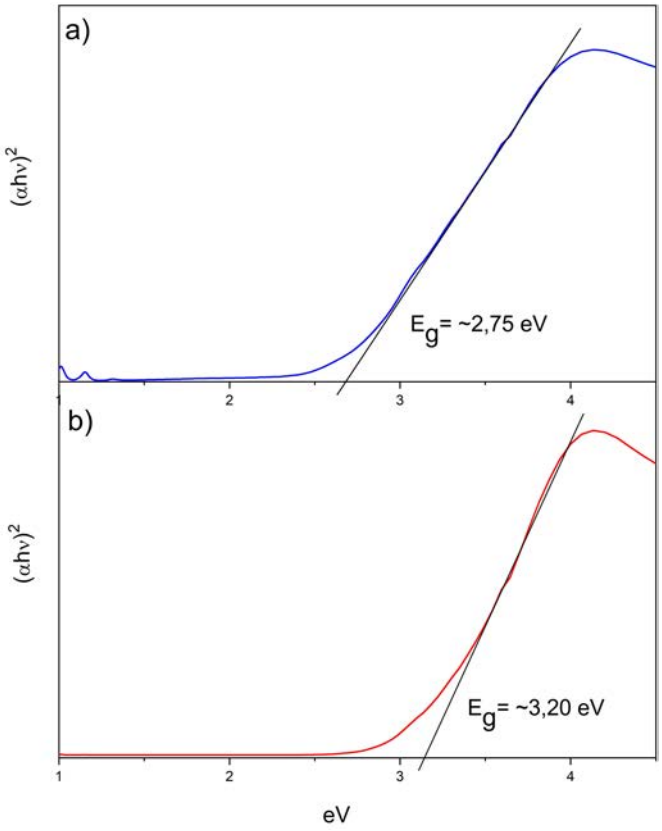

Figure 8. Kubelka–Munk transformation of UV–VIS–DRS spectra of Sm_5VO_{10} obtained with the methods: a) high-temperature, b) mechanochemical.

Based on the analysis of the transformed reflection spectrum of pentasamarium decaoxovanadate, it was determined that this compound is characterised by an energy gap with a value of about 3 eV, which classifies it in the group of wide gap semiconductors. Sm_5VO_{10} obtained with the high-temperature method (Fig. 8a) is a semiconductor with $E_g \sim 2.75$ eV, and the same compound obtained with the mechanochemical method (Fig. 8b), which is a semiconductor with $E_g \sim 3.2$ eV. These differences result from the dependence of some physicochemical properties on the size of the crystallites (Jain and Arun, 2013; Malicka et al., 2020). Grain size, especially its reduction to the nanoscale, can affect the mechanical properties of the material as well as the electrical and magnetic properties (Malicka et al., 2020). Generally, as the grain size of the material decreases, the energy of the bandgap increases. This is due to the influence of the size of the crystallites on the degree of their defect. Smaller grains have a greater number of defects, which increases the energy of the bandgap.

The established broad physicochemical characteristics of the compound Sm_5VO_{10}, and in particular the estimated value of its energy gap, indicate that the title compound may in future find application as, inter alia, a photocatalyst for water purification and in the production of optoelectronic devices, e.g. photodetectors, crystal lasers, light emitting diodes. Such devices are used in measuring apparatus, automation, data processing technology, memory systems, radiolocation equipment, etc.

Research to confirm the potential application of the compound Sm_5VO_{10} will be continued. It has not been planned as part of this paper due to its broad character and its separate nature. It will form the content of a separate scientific paper.

4. CONCLUSIONS

Results of the study showed that:

- Compound Sm_5VO_{10} formed in the binary oxide system V_2O_5–Sm_2O_3 can be synthesized both with high-temperature synthesis (microcrystalline) and mechanochemical method (nanocrystalline).
- The synthesis of Sm_5VO_{10} occurs through intermediate steps where $SmVO_4$ or $Sm_8V_2O_{17}$ are formed.
- Sm_5VO_{10} obtained with high-temperature method, crystallizes in monoclinic system; calculated unit cell parameters are as follows: $a = 0.9041$ nm, $b = 0.8022$ nm, $c = 1.3239$ nm, $\beta = 90.7148°$. Number of molecules in the unit cell $Z = 4$.
- Structure of the compound Sm_5VO_{10} is made up of foremost VO_4 tetrahedra and SmO_8 dodecahedra.
- Compound Sm_5VO_{10} is thermally stable in the air atmosphere up to around 1475 °C, and then it decomposes in the solid state, giving Sm_2O_3 and $Sm_8V_2O_{17}$.
- Depending on the synthesis method, energy band gap values are $E_g \sim 2.75$ eV (for Sm_5VO_{10} obtained with high-temperature method) and $E_g \sim 3.20$ eV (for that synthesized with high-energy ball milling method).
- E_g values indicate, that regardless of the synthesis method, compound Sm_5VO_{10} belongs to the wide group of gap semiconductors.

REFERENCES

Au C.T., Zhang W.D., Wan H.L., 1996. Preparation and characterization of rare earth orthovanadates for propane oxidative dehydrogenation. *Catal. Lett.*, 37, 241–246. DOI: 10.1007/bf00807761.

Balaram V., 2019. Rare earth elements: A review of applications, occurrence, exploration, analysis, recycling, and environmental impact. *Geosci. Front.*, 10, 1285–1303. DOI: 10.1016/j.gsf.2018.12.005.

Baláž P., Achimovičová M., Baláž M., Billik P., Cherkezova-Zheleva Z., Criado J.M., Delogu F., Dutková E., Gaffet E., Gotor F.J., Kumar R., Mitov I., Rojac T., Senna M., Streletskii A., Wieczorek-Ciurowa K., 2013. Hallmarks of mechanochemistry: from nanoparticles to technology. *Chem. Soc. Rev.*, 42, 7571–7637. DOI: 10.1039/c3cs35468g.

Brusset H., Madaule-Aubry F., Blanck B., Glaziou J.P., Laude J.P., 1971. Etude des oxydes mixtes de lanthanides et de vanadium(V). *Can. J. Chem.*, 49, 3700–3707. DOI: 10.1139/v71-617.

Chakoumakos B.C., Abraham M.M., Boatner L.A., 1994. Crystal structure refinements of zircon-type MVO_4 (M = Sc, Y, Ce, Pr, Nd, Tb, Ho, Er, Tm, Yb, Lu). *J. Solid State Chem.*, 109, 197–202. DOI: 10.1006/jssc.1994.1091.

Denisova L.T., Kargin Y.F., Chumilina L.G., Denisov V.M., Istomin S.A., 2015. Heat capacity and thermodynamic properties of the $SmVO_4$ orthovanadate in the range 369–1020 K. *Inorg. Mater.*, 51, 675–679. DOI: 10.1134/S0020168515060035.

Dunkle S.S., Helmich R.J., Suslick K.S., 2009. $BiVO_4$ as a visible-light photocatalyst prepared by ultrasonic spray pyrolysis. *J. Phys. Chem. C*, 113, 11980–11983. DOI: 10.1021/ jp903757x.

Filipek E., Wieczorek-Ciurowa K., 2009. Comparison between the synthesis in molybdenum and antimony oxides system by high-temperature treatment and high-energy ball milling. *J. Therm. Anal. Calorim.*, 97, 105–110. DOI: 10.1007/s10973-009-0071-y.

Frederickson L.D., Hausen D.M., 1963. Infrared spectra–structure correlation study of vanadium-oxygen compounds. *Anal. Chem.*, 35, 818–827. DOI: 10.1021/ac60200a018.

Gao J., Zhao Y., Yang W., Tian J., Guan F., Ma Y., Hou J., Kang J., Wang Y., 2003. Preparation of samarium oxide nanoparticles and its catalytic activity on the esterification. *Mat. Chem. Phys.*, 77, 65–69. DOI: 10.1016/S0254-0584(01)00594-6.

Gao L., Wong S.T.C., 2014. Chapter 11 – Label-free molecular vibrational imaging for cancer diagnosis, In: Chen X., Wong S. (Eds.), *Cancer Theranostics*. Academic Press, San Diego, 187–199. DOI: 10.1016/B978-0-12-407722-5.00011-6.

Ge X., Zhang Y., Wu H., Zhou M., Lin T., 2018. $SmVO_4$ nanocrystals with dodecahedral shape: Controlled synthesis, growth mechanism and photoluminescence properties. *Mater. Res. Bull.*, 97, 81–88. DOI: 10.1016/j.materresbull.2017. 08.037.

Huang S., Wang X., Zhu Q., Li X., Li J.-G., Sun X., 2020. Systematic synthesis of $REVO_4$ micro/nano crystals with selective exposure of high energy {001}facets and luminescence (RE=lanthanide and $Y_{0.95}Eu_{0.05}$). *J. Mater. Res. Technol.*, 9, 12547–12558. DOI: 10.1016/j.jmrt.2020.09.006.

Jain P., Arun P., 2013. Influence of grain size on the band-gap of annealed SnS thin films. *Thin Solid Films*, 548, 241–246. DOI: 10.1016/j.tsf.2013.09.089.

Kitayama K., Katsura T., 1977. Phase equilibria in Sm_2O_3–V_2O_3–V_2O_5 system at 1200 °C. *Bull. Soc. Chim. Jap.*, 50, 889–894. DOI: 10.1246/bcsj.50.889.

Kubelka P., Munk F., 1931. Ein Betrag zur Optik der Farbanstriche. *Z. Tech. Phys.,* 12, 593–601.

Li T., He Y., Lin H., Cai J., Dong L., Wang X., Luo M., Zhao L., Yi X., Weng W., 2013. Synthesis, characterization and photocatalytic activity of visible-light plasmonic photocatalyst AgBr-$SmVO_4$. *Appl. Catal. B*, 138–139, 95–103. DOI: 10.1016/j.apcatb.2013.02.024.

Malicka E., Karolus M., Panek J., Stokłosa Z., Groń T., Gudwański A. , Sawicki B., Goraus J., 2020. Effect of crystallite size on electrical and magnetic properties of $CuCr_2S_4$ nanoparticles obtained by mechanical alloying from sulphides. *Physica B,* 581, 411829. DOI: 10.1016/j.physb.2019.411829.

Patterson A.L., 1939. The Scherrer formula for X-ray particle size determination. *Phys. Rev.*, 56, 978–982. DOI: 10.1103/PhysRev.56.978.

Piz M., Dulian P., Filipek E., Wieczorek-Ciurowa K., Kochmański P., 2018. Characterization of phases in the V_2O_5–Yb_2O_3 system obtained by high-energy ball milling and high-temperature treatment. *J. Mater. Sci.*, 53, 13491–13500. DOI: 10.1007/s10853-018-2449-3.

Piz M., Filipek E., 2017. Synthesis and homogeneity range of $Yb_{8-x}Y_xV_2O_{17}$ in the $Yb_8V_2O_{17}$–$Y_8V_2O_{17}$ system. *J. Therm. Anal. Calorim.*, 130, 277–283. DOI: 10.1007/s10973-017-6379-0.

Rahimi-Nasrabadi M., Pourmortazavi S.M., Aghazadeh M., Ganjali M.R., Karimi M.S., Novrouzi P., 2017. Samarium carbonate and samarium oxide; synthesis, characterization and evaluation of the photo-catalytic behavior. *J. Mater. Sci.: Mater. Electron.*, 28, 5574–5583. DOI: 10.1007/s10854-016-6224-4.

Remizov V.G., Molodkin A.K., Skorikov V.M., 1976. Sistemi oksid vanadia(V)–oksid neodyma i oksid vanadia(V)–oksid samaria. *Zh. Neorg. Khim.*, 21, 1323–1327.

Sriram B., Baby J.N., Hsu Y., Wang S., George M., 2023. Scheelite-type rare earth vanadates TVO_4 (T=Ho, Y, Dy) electrocatalysts: Investigation and comparison of T site variations towards bifunctional electrochemical sensing application. *Chem. Eng. J.*, 451, 138694. DOI: 10.1016/j.cej.2022.138694.

Tojo T., Zhang Q., Saito F., 2007. Mechanochemical synthesis of rare earth orthovanadates from R_2O_3 (R=rare earth elements) and V_2O_5 powders. *J. Alloys Compd.,* 427, 219–222. DOI: 10.1016/j.jallcom.2006.02.052.

Yamaguchi O., Mukaida Y., Shigeta H., Takemura H., Yamashita M., 1989. Preparation of alkoxy-derived yttrium vanadate. *J. Electrochem. Soc.*, 136, 1557–1560. DOI: 10.1149/1.2096960.

Zhang Q., Saito F., 2000. Mechanochemical synthesis of lanthanum aluminate by grinding lanthanum oxide with transition alumina. *J. Am. Ceram. Soc.,* 83, 439–441. DOI: 10.1111/j.1151-2916.2000.tb01215.x.

Zhang Q., Saito F., 2012. A review on mechanochemical syntheses of functional materials. *Adv. Powder Technol.,* 23, 523–531. DOI: 10.1016/j.apt.2012.05.002.